

# AN INVESTIGATION OF MODE I FRACTURE TOUGHNESS USING ALIGNED CARBON NANOTUBE FORESTS AT THE CRACK INTERFACE

**R. Radjef\*, B.G. Falzon\*<sup>1</sup>, S.C. Hawkins\*\***

**\*Department of Mechanical & Aerospace Engineering, Monash University, VIC, 3800, Australia**

**\*\*CSIRO Materials Science and Engineering, Clayton, VIC, 3168, Australia**

<sup>1</sup>*Brian.Falzon@monash.edu*

**Keywords:** *carbon fibre composites, aligned CNTs, Mode I tests, fracture toughness*

## Abstract

*This paper presents a novel approach for introducing aligned carbon nanotubes (CNTs) at the crack interface of pre-impregnated (pre-preg) carbon fibre composite plies, creating a hierarchical (three-phase) composite structure. The aim of this approach is to improve the interlaminar fracture toughness. The developed method for transplanting the aligned CNTs from the silicon wafer onto the pre-preg material is described. Scanning electron microscopy (SEM) was used to analyse the effects of the transplantation method. Double Cantilever Beam (DCB) specimens were prepared, according to ASTM standard D5528-01R07E03 [1] and aligned multi-walled carbon nanotubes (MWCNTs) were introduced at the crack-tip. Mode I fracture tests for pristine (control) specimens and CNT-enhanced specimens were conducted and an average increase in the critical strain energy release rate ( $G_{Ic}$ ) of approximately 50 % was achieved.*

## 1 Introduction

CNTs have received considerable attention in the field of carbon fibre reinforced polymers (CFRP) over the last two decades due to their incredible material properties [2]. Reported measurements of Young's modulus range from 0.32 TPa to 1.47 TPa while the reported CNT strength varies between 0.01 TPa and 0.06 TPa

[3]. While challenges to creating CNT fibres as the primary reinforcement remains, their utilization to improve the fracture toughness of the matrix has received considerable attention [4]. The relatively low through-thickness strength of the epoxy resin leads to low values of fracture toughness. The introduction of CNTs in the matrix has proceeded along a number of fronts [5, 6]. Most studies were performed with CNTs randomly dispersed in the resin, using mechanical mixing or sonication, for subsequent vacuum-assisted resin infusion (VARTM) of a carbon fibre preform. The results have been shown to be highly variable and the expected large increase in structural performance has not been realized, at least, not consistently. By introducing the CNTs into the matrix in the form of an aligned CNT forest, a hierarchical composite with through-thickness reinforcement, analogous to stitching or z-pinning can potentially lead to structural enhancements without the well-documented drawbacks associated with the afore-mentioned through-thickness enhancement techniques. It is acknowledged that Garcia et al. [7] presented another approach for transferring a CNT forest onto a laminate. Attempts at growing CNTs onto alumina fibres have also been reported by the same research group [8] but this approach is unlikely to be suitable for carbon-fibres because of the high temperatures involved in the production of CNTs.

## 2 Experimental

A novel transplantation method for aligned CNTs is presented followed by the preparation of the double cantilever beam (DCB) specimens. Scanning electron microscopy (SEM) was used to verify alignment after the transplantation process.

### 2.1 Transplantation of the CNTs

The CNT forests were produced at CSIRO in Melbourne using a Chemical Vapour Deposition (CVD) process [9, 10]. A three-zone furnace with a heated length of 400 mm in combination with a quartz tube with an inside diameter of 90 mm was used. Acetylene with a concentration of 2.4 % (100 sccm) was used with a Helium carrier at a concentration of 96 % (4000 sccm). The reaction time for the synthesis was set to 20 min with a plateau temperature of 680°C. The CNTs were grown on a semiconductor grade Silicon substrate with a 50 nm thick thermal oxide layer and a

2.3 nm thick iron catalyst coating that was deposited by using e-beam evaporation. Scanning electron microscopy (SEM) as well as transmission electron microscopy (TEM) were used to observe the morphology of the CNTs. The provided CNTs had an average length of 100-200  $\mu\text{m}$  and were made up of 7  $\pm$  2 walls which corresponds to a diameter of approximately 10 nm. TEM images revealed a minimal amount of amorphous carbon and no particulated iron for the produced CNTs.

Transplantation of the forests from the silicon-wafer onto the carbon fibre prepreg was an investigation process that involved the trial of different techniques with the goal of achieving a complete transplantation of the CNTs. Samples of various shapes were used for a transplantation approach based on heat and pressure which increased the tackiness of the prepreg and allowed capillary forces to infuse the resin into the forest as well as promote partial penetration of the forest into the ply.

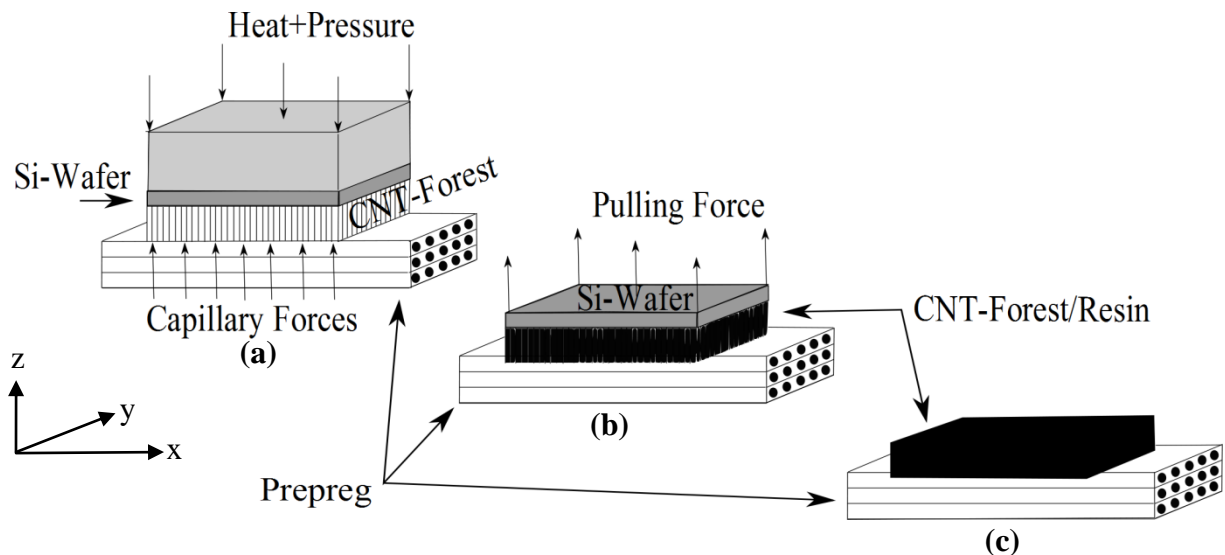


**Fig. 1:** Transplantation process using heat and pressure (a) heated weight placed on top of the silicon wafer and capillary forces infuse resin into the CNT-forest (b) removal of the silicon wafer after the cool down period (c) transplanted CNT forest infused with resin and partially inserted into the pre-preg.

A series of tests were conducted to explore a suitable combination of heat and pressure to achieve complete transplantation of the forest as well as partial penetration of the forest into the pre-preg laminate. Two different types of specimens were produced to analyse the effects

of the transplantation method. For the first set of specimens a CNT forest was transplanted onto a single pre-preg ply with the purpose of verifying complete wetting of the forest with the resin available from the pre-preg. The silicon wafer containing the "as-grown" CNT

forest was inverted and placed onto the laminate. A heated weight was placed on the wafer for a specified period of time and then removed along with the wafer, Fig. 1.

Extensive scanning electron microscopy (SEM) was performed to observe the interaction of the CNTs with the carbon fibres and the wetting of the CNTs. Fig. 2 shows the SEM image of a CNT forest transplanted onto a single prepreg ply.

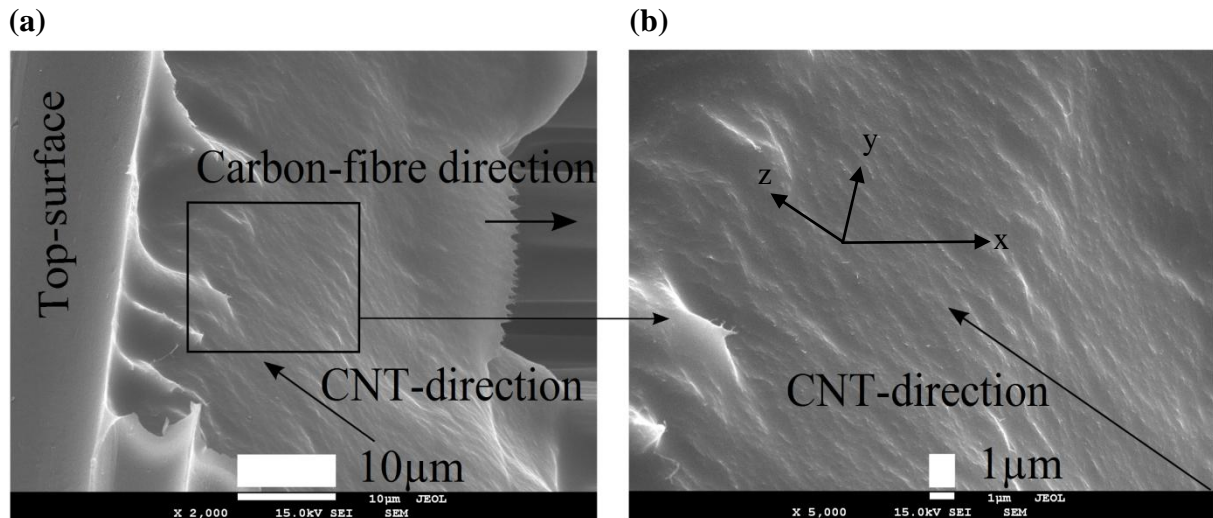


**Fig. 2:** SEM images of the right edge of sample 3 (a) part of the top-surface, the edge of the CNT forest and part of the pre-preg ply with a visible carbon fibre (b) close-up of the edge of the CNT forest showing the CNT direction and complete wetting.

In order to visualize the CNTs it was necessary to look at the edge of the CNT forest. Complete wetting of the forest, through capillary action, was achieved with the resin provided by a single pre-preg ply. The alignment of the CNTs was not disturbed by the transplantation method, Fig. 2(b). The structured appearance of the resin is due to the embedded CNTs. In reality, aligned CNTs are not perfectly straight as is evident by the slight waviness observed in the images. After complete wetting of the CNT forest was ensured, they were introduced into the mid-plane of a laminate in order to analyse the interactions between CNTs and carbon-fibre pre-preg, regarding the penetration and alignment of the forest. A pre-preg plate was manufactured and samples for analysis using

SEM were cut out using a waterjet cutter. Fig. 3 shows the SEM image of a CNT forest introduced into the mid-plane. The images show that the alignment of CNTs remained once introduced into the mid-plane. The penetration of the CNTs into the pre-preg cannot be seen on the basis of this image thus a different image of a cross-section was taken, Fig. 4. The images provide proof of the CNT forest partially penetrating the carbon-fibre pre-preg. When looking at the transition from CNT forest to pre-preg material it is obvious that the CNTs surround individual carbon fibres. A nano-enhanced resin rich region of approximately 100 µm was created by the introduced CNT forest.

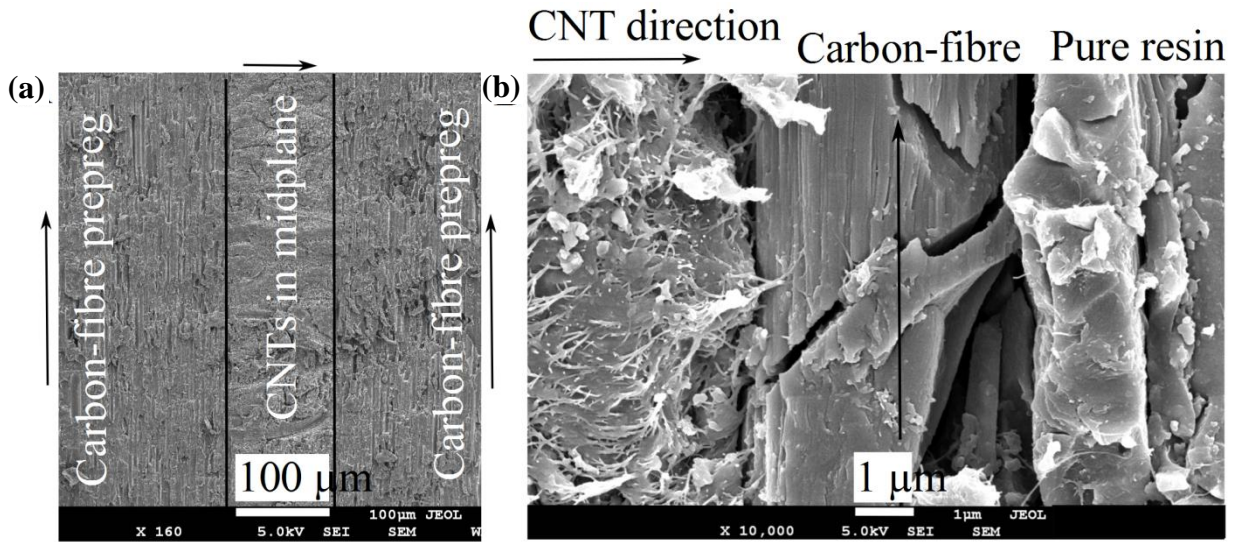


**Fig. 3:** Two SEM images showing the interaction of the CNT forest with the carbon fibres in the longitudinal direction (a) CNT forest transplanted into the mid-plane of a pre-preg plate (b) transition from CNT forest to carbon fibre pre-preg at high magnification - CNT forest on the left, a single carbon fibre in the middle and pure resin with CNTs on the right.

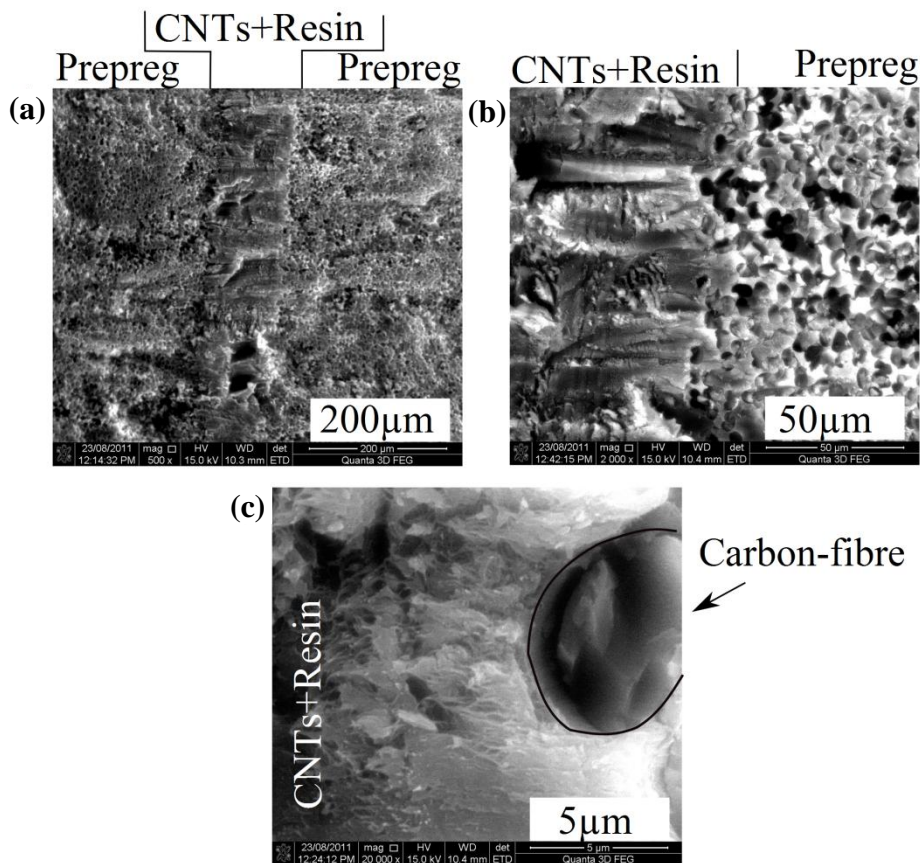


**Fig. 4:** Three SEM images showing the interaction of the CNT forest with the carbon fibres (a) CNT forest introduced in the mid-plane of a pre-preg plate and a nano-enhanced resin-rich region of approximately 100 μm (b) The right side of the CNT-forest at a higher magnification - partial penetration of the forest into the pre-preg (c) interaction of CNT forest and a single carbon fibre at another magnification level - CNTs surround the carbon fibre.

## 2.2 Manufacturing of the test specimens

Mode I specimens were produced according to ASTM standard D5528-01R07E03. A set of pristine specimens was manufactured as a reference to determine the change in fracture toughness caused by the introduction of the CNTs. A 200 mm x 200 mm pre-preg plate was manufactured by laying up nine plies of SE84LV/HSC unidirectional prepreg material from GURIT and placing a Teflon insert to create a starter crack. A second pre-preg plate containing nine plies was manufactured and placed on top of the first one, creating a pre-preg plate containing 18 plies and an 80 mm long pre-crack.

The manufacturing of the CNT-enhanced DCB specimens included the introduction of the CNT forest at the crack tip. The knowledge gained from the previous transplantation experiments was used to achieve complete transplantation. Six 25 mm x 25 mm silicon wafers were placed next to each other along the crack tip. The CNT forests on the silicon wafers had an average height of 100  $\mu\text{m}$ . After assembling the two pre-preg halves, the plate with the CNTs introduced in the mid-plane and the pristine plate were cured under vacuum in an oven at 92  $^{\circ}\text{C}$  for 10 h, following the manufacturer's recommendation. The DCB specimens of dimensions 160 mm x 20 mm were cut out of the plate. The average thickness of the specimens was 4 mm. After adhesively-bonding the loading hinges onto the specimens, an effective initiation crack length of approximately 50 mm was measured. White correction fluid was applied on the specimens' edges and marked with 1mm intervals to track the crack propagation as a function of loading.

## 2.3 Mode I fracture tests

Mode I tests were performed on an Instron 5848 MicroTester with a calibrated 2 kN load cell using displacement control with a constant speed of 0.5 mm/min. Load and displacement were recorded by the MicroTester with a resolution of 1  $\mu\text{N}$  and 1 nm respectively while two microscopic cameras on both sides of the installed specimen were used to trace the crack and record the crack growth until a crack length of 20 mm was reached. Two sets of DCB specimens were tested in order to compare the fracture behaviour: One set with and one set without aligned CNT forests introduced at the crack-tip.

## 3 Results and Discussion

A novel transplantation method for aligned CNT forests was successfully developed and confirmed using SEM. The presence of the CNTs resulted in a nano-enhanced resin-rich region which penetrated into the prepreg by approximately 5-10  $\mu\text{m}$ . This region may be reduced by using CNT forests of a lower height/thickness.

The production of CNT-enhanced DCB specimens containing aligned CNTs in the mid-plane was successful and Mode I fracture tests were performed. The average toughening curves for the pristine and CNT-enhanced DCB specimens are shown in Fig. 5. The pristine specimens had an average critical strain energy release rate  $G_{Ic} = 278.77 \text{ J/m}^2$ . The CNT-enhanced specimens had an average critical strain energy release rate  $G_{Ic} = 421.29 \text{ J/m}^2$  which corresponds to an increase of approximately 50 %. During the crack propagation of the CNT-enhanced specimens, crack bridging as well as crack propagation in multiple planes was observed in some specimens requiring further investigation of the fracture surfaces.

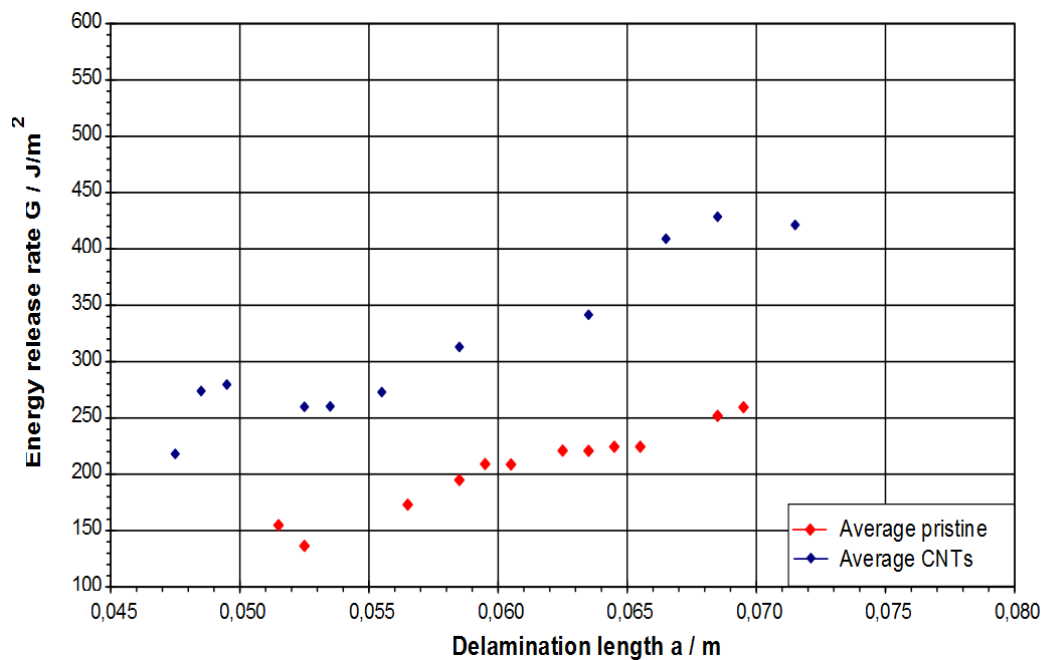


**Fig. 5:** R-curves of the pristine and CNT-enhanced DCB specimens.

The comparison of the average energy release rate at crack initiation showed a  $G_{Ic}$  of  $154.89 \text{ J/m}^2$  for the pristine specimens and a  $G_{Ic}$  of  $218.16 \text{ J/m}^2$  for the CNT enhanced specimens which corresponds to an increase of approximately 40 %. The fracture surfaces of the CNT enhanced specimens revealed different crack paths, characterised by partial propagation through the CNT forest and crack migration to the CNT-forest/ply interface suggesting that the penetration of the CNT forest through the pre-preg was not consistent during manufacture. Higher increases in strain energy release rates can be reasonably expected for crack propagation through the entire forest. Fig. 6 shows two SEM images of a fracture surface indicating a combination of partial horizontal crack propagation through the CNT forest region and crack migration to the CNT forest/pre-preg interface. The width of the CNT forest with horizontal crack propagation measured approximately 4 mm which equals 16% of the total width of the specimen. With reference to Fig. 6(a), the surface of the CNT region is covered with ridges at different depth levels which indicate a high amount of energy dissipation during the crack propagation process. In Fig. 6(b) a magnification of the right edge of the CNT-forest is shown. On the

left side, the fracture surface of the CNT area is visible. In this region, the crack path propagated through the CNT area as evident by the morphology of the crack surface and the exposed CNTs. The other half of the DCB specimen (not shown) also had a similar morphology which supports this hypothesis.

The surface roughness and depth levels on the fracture surface of the CNT forest explain the higher energy release rate for certain specimens. Nonetheless, the right hand side of this image does suggest some crack migration to the CNT forest/ply interface. The increase in fracture toughness for specimens showing this type of fracture surface was higher than for specimens with fracture surfaces shown in Fig. 7. A low magnification of the fracture surface is shown in Fig. 7(a) with the CNT-forest on the left side and the adjacent ply on the right side. The top and bottom edge of the forest are marked and a forest height of approximately  $100 \mu\text{m}$  is visible. The top of the CNT forest appears flat and smooth. On the right side of the image exposed carbon fibres are visible. In Fig. 7(b) the top-surface of the CNT-forest is visible and appears smooth without exposed CNT. This indicates that the crack travelled through the CNT forest/ply interface without causing fracture of the forest. The side-view of

## AN INVESTIGATION OF MODE I FRACTURE TOUGHNESS USING ALIGNED CARBON NANOTUBE FORESTS AT THE CRACK INTERFACE

the forest shows exposed CNTs that are still aligned which indicates that the crack migrated

through the CNT forest connecting the two fracture different planes.

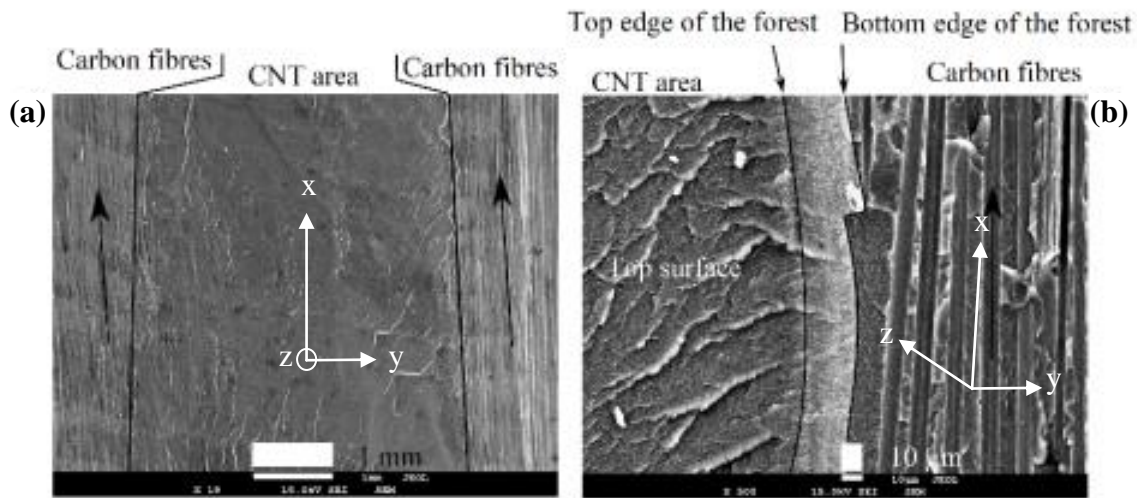


**Fig. 6:** Two SEM images of the fracture surface of CNT specimen 4 are presented (a) a region of CNT forest on top of the pre-preg is shown at low magnification. The carbon fibres are visible to the left and right of the CNT forest. The CNT region appears rough with ridges produced during the crack propagation (b) the right edge of the CNT forest with part of the pre-preg is shown at high magnification. The top of the CNT surface appears rough with different depth levels. At the transition from pre-preg to CNT forest, an area on top of the pre-preg is visible that is covered with CNTs.

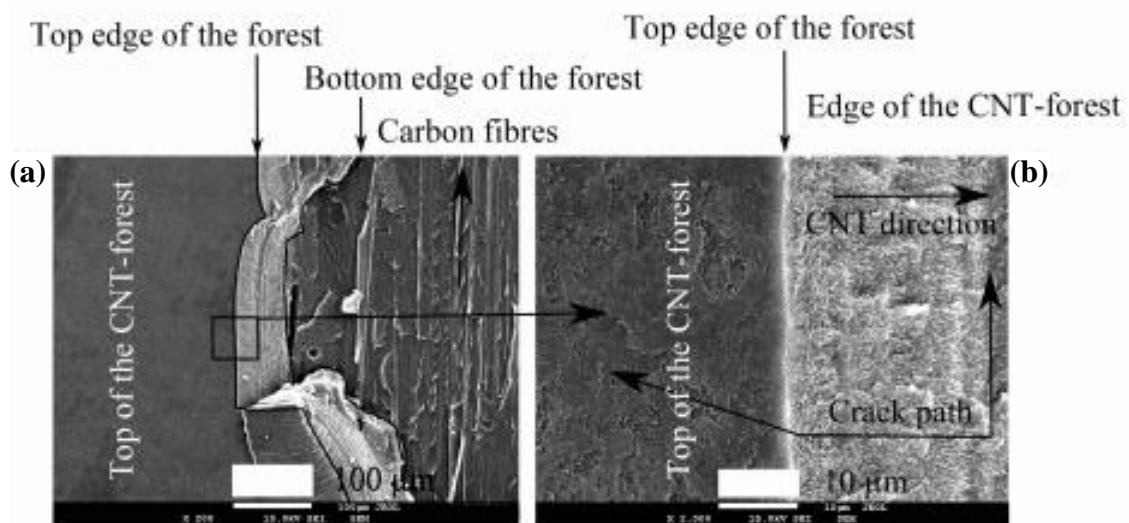


**Fig. 7:** Two SEM images of the fracture surface of CNT specimen 6 are presented (a) the top and side of the CNT forest as well as the ply at low magnification are visible. The top of the CNT forest appears smooth with no exposed CNTs (b) detail of top edge of CNT forest at higher magnification.

It is known from section 2 that the resin from the bottom pre-preg was infused into the CNT forest by capillary forces, wetting it completely. The relatively high temperature that was used for the transplantation process may have initiated a partial cure of the resin in the CNT forest, reducing its capacity to embed

itself in the other pre-preg half to create a strong CNT forest/ply interface.

### 3 Conclusion and Recommendation

The fabrication of double cantilever beam specimen with aligned CNTs at the crack tip was demonstrated. Complete wetting of the CNT forest was confirmed by scanning electron microscopy (SEM). The careful application of heat and pressure on the CNT forest showed penetration of the CNTs into the first layer of the carbon fibre pre-preg and SEM images revealed CNTs partially surrounding the carbon-fibres. The Mode I test results indicated an average increase in the strain energy release rate of approximately 50 % over the pristine specimens. SEM images of the CNT-specimens showed the presence of a nano-enhanced resin-rich region in the mid-plane caused by the forest thickness of approximately 100  $\mu\text{m}$  with only relatively small penetration being achieved. The fracture surfaces indicated a weak bond between one side of the prepreg plate and the CNT forest, for some specimens, possibly due to pre-curing of the resin infused into the CNT-forest during transplantation.

An optimum pressure/temperature ratio is required to mitigate the chance of pre-curing the resin inside the CNT forest. While initial results are promising, further work is required to improve the production process and undertake more extensive testing. Developing a reliable and proven technique for introducing aligned CNTs at ply interfaces could have practical utilisation in adhesively-bonded composite structures where additional through-thickness strength and toughness may be required.

The results and information gained from these primary test build the basis for future projects. Fine tuning of the transplantation method and the reduction of the CNT forest length are recommended to ensure a strong bond between the pre-preg and the CNT forest, through greater penetration, and to reduce the thickness of the nano-enhanced resin-rich region. The particular composite system used in this study only required an oven cure and vacuum. Future studies will look at autoclave-

cured composite systems where the higher pressures available may promote further CNT penetration into the adjoining plies. The production of the CNT forest may also be modified in a way that the adhesion between CNTs and the growth substrate is minimal. This will further facilitate the complete transplantation of the forest onto the composite plies.

### References

1. ASTM D5528 - 01(2007)e3, Standard Test Method for Mode I Interlaminar Fracture Toughness of Unidirectional Fiber-Reinforced Polymer Matrix Composites, ASTM International, West Conshohocken, PA, DOI: 10.1520/D5528-01R07E03, 2007.
2. Thostenson, E.T., Li, C., and Chou, T.-W., *Nanocomposites in context*. Composites Science and Technology, **65**(3-4):2005 p. 491-516.
3. Coleman, J.N., Khan, U., Blau, W.J., and Gunko, Y.K., *Small but strong: A review of the mechanical properties of carbon nanotube-polymer composites*. Carbon, **44**(9):2006 p. 1624-1652.
4. Andrews, R. and Weisenberger, M.C., *Carbon nanotube polymer composites*. Current Opinion in Solid State and Materials Science, **8**(1):2004 p. 31-37.
5. Hsieh, T., Kinloch, A., Taylor, A., and Kinloch, I., *The effect of carbon nanotubes on the fracture toughness and fatigue performance of a thermosetting epoxy polymer*. Journal of Materials Science, **46**(23):2011 p. 7525-7535.
6. Qian, H., Greenhalgh, E.S., Shaffer, M.S.P., and Bismarck, A., *Carbon nanotube-based hierarchical composites: a review*. Journal of Materials Chemistry, **20**(23):4751-4762.
7. Garcia, E.J., Wardle, B.L., and John Hart, A., *Joining prepreg composite interfaces with aligned carbon nanotubes*. Composites Part A: Applied Science and Manufacturing, **39**(6):2008 p. 1065-1070.
8. Garcia, E.J., Wardle, B.L., John Hart, A., and Yamamoto, N., *Fabrication and multifunctional properties of a hybrid laminate with aligned carbon nanotubes grown In Situ*. Composites Science and Technology, **68**(9):2008 p. 2034-2041.
9. Huynh, C.P. and Hawkins, S.C., *Understanding the synthesis of directly spinnable carbon nanotube forests*. Carbon, **48**(4):2010 p. 1105-1115.



10. Huynh, C.P., Hawkins, S.C., Redrado, M., Barnes, S., Lau, D., Humphries, W., and Simon, G.P., *Evolution of directly-spinnable carbon nanotube growth by recycling analysis*. Carbon, **49**(6)1989-1997.

### Copyright Statement

The authors confirm that they, and/or their company or organization, hold copyright on all of the original material included in this paper. The authors also confirm that they have obtained permission, from the copyright holder of any third party material included in this paper, to publish it as part of their paper. The authors confirm that they give permission, or have obtained permission from the copyright holder of this paper, for the publication and distribution of this paper as part of the ICAS2012 proceedings or as individual off-prints from the proceedings.